

Radially Self-Accelerating Beams

Christian Vetter, Toni Eichelkraut, Marco Ornigotti, Markus Gräfe, and Alexander Szameit*
Institute of Applied Physics, Friedrich-Schiller-Universität Jena, Germany

(Dated: April 22, 2021)

We report on optical non-paraxial beams that exhibit a self-accelerating behavior in radial direction. Our theory shows that those beams are solutions to the full scalar Helmholtz equation and that they continuously evolve on spiraling trajectories. We provide a detailed insight into the theoretical origin of the beams and verify our findings on an experimental basis.

PACS numbers: 42.25.Fx, 42.25.Hz, 42.60.-v

Self-accelerating wave packets freely accelerate even without any external potential present. This intriguing phenomenon is of rapidly growing interest since its advent in optics in 2007 [1–6]. The most prominent example of self-accelerating waves has been introduced by Siviloglou and coworkers [1, 2]: They demonstrated, that an Airy-type wave packet exhibits a linear transversal acceleration and is therefore following a parabolic trajectory.

Enlarging the scope and the versatility of Airy beams, nonparaxial generalizations in terms of full vectorial solutions of Maxwell’s equations [7] as well as by the method of caustics [8] were investigated. Their curved trajectories render classical Airy beams a powerful tool in many areas of application. For instance, in the field of particle manipulation, micro beads have been guided and sorted in a new fashion [9] beyond the scope of classical optical tweezers. Moreover, it was shown that curved plasma channels have many advantages over their straight counterparts, e.g., when it comes to the spatially resolved detection of secondary signals [10]. Additionally, Airy wave packets inspired excessive fundamental research in the field of nonlinear optics [11–14], and boosted the study of waves with intensity maxima that propagate along almost arbitrary trajectories [15]. Broadening the range of influence beyond the scope of optics, Airy beams have been utilized in electron beam shaping [16] as well.

One common feature of all of the aforementioned waves - even in two-dimensional settings - is that they acceler-

ate linearly, namely along a specific Cartesian coordinate axis (see Fig. 1 (a)). This obvious limitation brings about a number of fundamental questions: Is it possible to generate optical beams that show a self-accelerating behavior along different types of trajectories? Could such wave packets be shape-invariant or even non-diffractive? Based on the numerous already existing applications of Airy-type beams discussed in the previous paragraph, it should be obvious that beams for which the aforementioned questions can be answered affirmatively would enrich the optical toolbox in many areas of application and research. Moreover, from a fundamental point of view, it is essential to determine under which kind of approximations analytical solutions for such beams can be found. In other words, will those solutions be restricted to the paraxial case or do they obey the scalar Helmholtz equation or even Maxwell’s equations?

In the present article, we report on a new class of self-accelerating diffraction-free waves that move along three-dimensional spiraling trajectories. As such, they behave as if they were influenced by a radially symmetric external potential even though the propagation takes place in free space. Observed from a rotating, co-moving frame of reference like the one depicted in Fig. 1 (b), the beams we present are propagation-invariant. Within a thorough theoretical discourse we will derive a general, explicit, and analytical expression for this new class of beams. We will show the great versatility of these beams, for which - while outperforming Airy-type beams - the transverse cross-section is highly tunable after fixing predefined spiraling properties. In addition, we are going to verify our theoretical findings on an experimental basis utilizing an intuitive understanding borrowed from Fourier-optics. In this regard, we present a simple yet powerful setup that enables one to address the entire parameter range of the presented beams.

Our theoretical section is comprised of two parts. The first one consists of an extensive theoretical derivation regarding the most general expression of a beam which exhibits a field pattern that is invariant in a rotating frame of reference. As it will be discussed later, of more practical interest might be the implementation of beams with a rotating intensity distribution. For this reason, in the second part of our theory section, we pose conditions

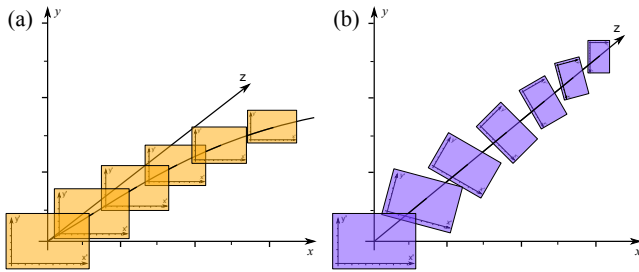


Figure 1. Illustrative presentation showing the accelerative behavior of Airy beams (a) and radially self-accelerating field/intensity distributions (b).

on the beam intensity only (i.e., no condition is posed on the phases) finding a more general class of beams.

First, we want to model a beam that is propagation-invariant in a co-moving, rotating frame. This wave is supposed to be a solution to the scalar Helmholtz equation $\Delta E + k^2 E = 0$, where E is a scalar electric field and $k = 2\pi/\lambda$ the corresponding wave number. Since we are dealing with rotating solutions, it is a natural choice to work with cylindrical coordinates. Then, the most general solution of the scalar Helmholtz equation can be written as

$$E(r, \varphi, z) = \sum_{n=-\infty}^{\infty} \int_0^{\infty} d\alpha C_n(\alpha) J_n(\alpha r) e^{i(n\varphi + \beta z)}, \quad (1)$$

which is essentially a superposition of fundamental eigenmodes given in terms of diffraction-free Bessel waves. The spatial structure of each eigenmode is determined by $J_n(\alpha r) e^{i(n\varphi + \beta z)}$, where $J_n(\alpha r)$ represents the Bessel function of order n and $\beta = \sqrt{k^2 - \alpha^2}$ is the longitudinal component of the wave vector, or propagation constant. For an arbitrary beam, the expansion coefficients $C_n(\alpha)$ are arbitrary as well. In the following, we will derive conditions for $C_n(\alpha)$ in order to obtain rotating self-similar solutions to the scalar Helmholtz equation. Note, that we restrict our analysis to beams that are propagating in the positive z -direction.

For a beam that is self-accelerating three major properties need to be fulfilled. First, no external potential or non-linear optical effect should be present. Second, the beam is diffraction-free in a certain frame of reference. Finally, an observer resting in the aforementioned reference frame would experience a fictitious force. The first condition is fulfilled immediately as we start our analysis from the linear and time-independent scalar Helmholtz equation. For the second requirement, a coordinate transformation needs to exist with which the field distribution is no longer dependent on the propagation direction. It can easily be shown that an electric field of the general form

$$E(r, \varphi, z) \stackrel{!}{=} E(r, \varphi + \omega z) \quad (2)$$

fulfils this condition. Obviously, with the substitution $\varphi' = \varphi + \omega z$ the field $E(r, \varphi')$ in Eq. (2) is no longer dependent on the longitudinal position z and thus remains unchanged for every z . Moreover, the aforementioned coordinate transformation describes a reference frame which is rotating with an angular velocity ω . As a consequence, the last requirement is satisfied, as an observer resting in this rotating frame of reference experiences a centrifugal force.

Since Eq. (2) has to hold for every φ and z , from Eq. (1) it immediately follows that

$$\beta/n \stackrel{!}{=} \omega. \quad (3)$$

As β was restricted to be positive, the first conclusion from condition (3) is that the signs of n and ω have to be equal, i.e., $\text{sign}(n) = \text{sign}(\omega)$. Moreover, since the propagation constant β is a function of the transverse component of the wave vector α , condition (3) can be rewritten as

$$\alpha \stackrel{!}{=} \alpha_n = \sqrt{k^2 - \omega^2 n^2} \quad (4)$$

Obviously, this restriction can only be fulfilled for the specific choice of coefficients

$$C_n(\alpha) = \tilde{C}_n \delta(\alpha - \alpha_n). \quad (5)$$

Applying the restrictions on $\text{sign}(n)$ as well as on $C_n(\alpha)$, Eq. (1) becomes

$$E(r, \varphi, z) = \sum_{n=1}^{n_{\max}} \tilde{C}_n J_n(\alpha_n r) e^{i(\text{sign}(\omega)n(\varphi + \omega z))}. \quad (6)$$

This is the most general expression of a beam that rotates in a shape-invariant fashion with an angular velocity ω . Note, that $n_{\max} = \max\{n \in \mathbb{N} : k^2 > \omega^2 n^2\}$ in order to ensure that evanescent waves are excluded from the sum. To give an intuitive description of this finding, it is helpful to consider the Fourier-transform of this specific field. In essence, the Fourier-transform is a discrete superposition of concentric rings with radius α_n whereas the amplitude of these rings is given by the coefficients \tilde{C}_n . Note that for a given ω Eq. (5) states that for each order n there is exactly one ring radius α_n . Moreover, each ring of order n carries a helical phase pitch of $2\pi n$.

The field pattern of a beam described by Eq. (6) gives rise to screw-shaped trajectories, that show a non-degenerate periodicity in the azimuthal and the propagation direction. Figure 2 shows an appropriate example using four Bessel waves ranging from order 1 to 4, i.e., $\tilde{C}_n = 1$ for $1 \leq n \leq 4$ and $\tilde{C}_n = 0$ for $n > 4$. The depicted insets emphasize the fact that amplitude and phase are rotating synchronously as predicted. The angular frequency spectrum consists of four concentric rings with radii determined by Eq. (4).

At the beginning of the theory section we indicated that for many practical applications, such as optical tweezing or micro-fabrication, only the intensity distribution of a beam might be of interest. For this reason, we want to state how the requirements for the beam profile change if condition (2) is posed on the intensity, i.e., $I(r, \varphi, z) = |E(r, \varphi, z)|^2 = I(r, \varphi + \omega z)$. It will be shown that this scenario is more general and offers a larger degree of freedom. Consequently, in our subsequent discussion (including our experimental section) we will exclusively concentrate on this more general case. As the derivation of the following results is somewhat more lengthy and does not convey much additional physical insight, it is contained in the Supplementary Material.

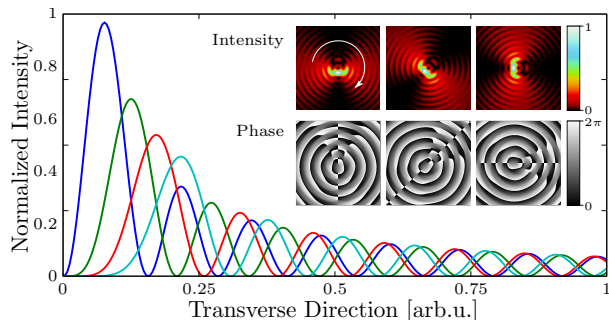


Figure 2. Exemplary illustration of a radially self-accelerating field distribution with $\tilde{C}_n = 1$ for $1 \leq n \leq 4$ and $\tilde{C}_n = 0$ for $n > 4$. The figure consists of 1-dimensional representation of the superimposed Bessel functions (main plot), resulting intensity distribution (upper inset row) and resulting phase pattern (lower inset row).

However, from this derivation, one arrives at a constrain similar to (4), which reads

$$\alpha_n = \sqrt{k^2 - (\omega n + \beta_0)^2}. \quad (7)$$

Moreover, under these conditions the field is given by

$$E(r, \varphi, z) = e^{i\beta_0 z} \sum_{n \in \mathcal{N}} \tilde{C}_n J_n(\alpha_n r) e^{i(n(\varphi + \omega z))}. \quad (8)$$

Note that there are two main differences between Eq. (8) and Eq. (6). The first difference is that Eq. (8) contains the global phase factor $e^{i\beta_0 z}$ with the propagation constant β_0 , which can be regarded as a free parameter for these beams. Consequently, one can already see that the field given by Eq. (8) does not fulfill the requirement of a rotation invariant field anymore (only the intensity is rotation invariant). It is important to be aware of the fact that β_0 does not only determine the global phase factor but poses an important degree of freedom for scaling the transverse beam properties after fixing the rotation parameter ω . This becomes apparent when comparing Eq. (4) and Eq. (7). The second difference is that the sum in Eq. (8) contains also negative n , whereas Eq. (6) covers only positive n . To be specific, the set $\mathcal{N} = \{n \in \mathbb{Z} : k^2 > (\omega n + \beta_0)^2\}$ contains all integer numbers n for which Eq. (7) yields real values for α_n .

Please note that rotating intensity distributions based on pairs of superimposed Bessel-functions have been investigated theoretically and experimentally [17–25]. Our theory, however, describes rotating field/intensity patterns that are composed of an arbitrary number of Bessel waves. The arising enlarged degree of freedom renders useful when modeling specific beam properties as will be discussed in the upcoming paragraph. Figure 3 shows an exemplary beam with $\tilde{C}_n = 1$ for $-1 \leq n \leq +1$ and $\tilde{C}_n = 0$ for $|n| > 1$. The depicted insets demonstrate that the intensity distribution is indeed rotating during propagation while the corresponding phase is no longer

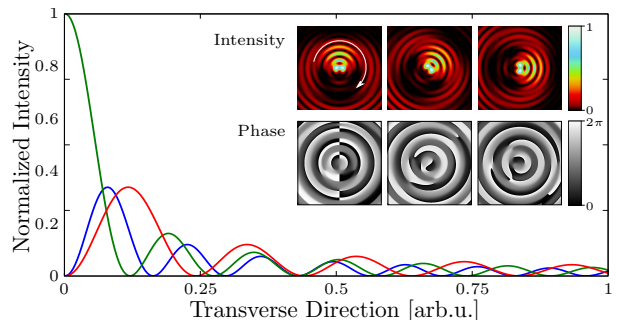


Figure 3. Exemplary illustration of a radially self-accelerating intensity distribution with $\tilde{C}_n = 1$ for $-1 \leq n \leq +1$ and $\tilde{C}_n = 0$ for $|n| > 1$. The figure consists of 1-dimensional representation of the superimposed Bessel functions (main plot), resulting intensity distribution (upper inset row) and resulting phase pattern (lower inset row).

synchronized. The angular frequency spectrum of the shown beam consists of three concentric rings with radii that are determined by Eq. (7).

An important, yet open question is how versatile the transverse cross-section of beams described by Eq. (8) can be tailored. In order to answer this question consider Eq. (8) in the initial plane ($z = 0$). For a given distance R from the origin of the coordinate system, Eq. (8) can be written as

$$E(R, \varphi, 0) = \sum_{n \in \mathcal{N}} D_n e^{in\varphi}, \quad (9)$$

where $D_n = \tilde{C}_n J_n(\alpha_n R)$. If the distance R is chosen such that $J_n(\alpha_n R) \neq 0$, then Eq. (9) represents a general Fourier-series. As an important consequence, the transverse beam profile can be tailored in a way that the field distribution on a circle with radius R can be chosen arbitrarily, in other words $E(R, \varphi, z = 0) = f(\varphi)$, where the complex function $f(\varphi)$ can be set without any condition. From this it follows that a cooking recipe to tailor these kind of rotating beams could be to fix the parameter β_0 as well as the function $f(\varphi)$. Then Eq. (7) determines α_n and the expansion coefficients are given by

$$\tilde{C}_n = \frac{1}{2\pi J_n(\alpha_n R)} \int_0^{2\pi} f(\varphi) e^{-in\varphi} d\varphi. \quad (10)$$

Note that as soon as the field is specified for one radius R , the entire field in the transverse plane is determined. This is simply due to the fixed radial dependence of the Bessel functions.

In order to experimentally implement our findings, we make use of the fact that the presented beams show a multi-ring pattern with distinct helical phase pitch in the angular frequency domain. Fourier transforming this pattern by means of a conventional lens will match the previously discussed theory. For the experimental setup,

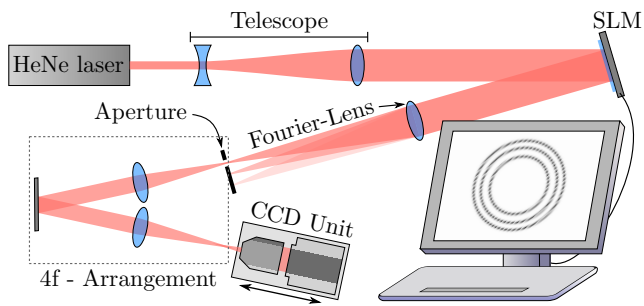


Figure 4. Experimental setup containing a telescope for beam expansion, SLM (Holoeye Pluto VIS) for amplitude and phase modulation, lens for Fourier transformation ($f = 300$ mm), aperture and 4f-arrangement ($f_1 = f_2 = 200$ mm) for signal cleaning as well as a movable CCD Unit (Basler Ace1600-20gm with Olympus Plan N 20 \times) for data acquisition.

different approaches are conceivable ranging from the use of axicons (conical lenses), ring slit apertures and phase plates to the exclusive use of spatial-light-modulators (SLMs). In this work, we followed this last approach as it provides the highest amount of flexibility. Our setup is presented in Fig. 4 and makes use of a technique introduced in Ref. [26]. This technique enables simultaneous amplitude and phase modulation with a single phase-only SLM by multiplying the desired amplitude distribution with a blazed grating. In our case this desired amplitude distribution is given by concentric rings - in other words, as previously mentioned, we implement the Fourier-transform of the desired beam in the SLM-plane. After the Fourier-transforming lens, undesired grating orders are filtered by a pin-hole and the primary signal is imaged by an additional 4f-setup. Finally, a movable CCD-camera allows to measure the change of the intensity profile in propagation direction.

With the proposed setup, we are able to cover almost the entire parameter range provided by our theory. This of course would go beyond the scope of this letter. We will therefore present an exemplary set of parameters upon which we show the practicability of radially self-accelerating beams and discuss the experimental limitations. One of these limitations is already given by the fact that Bessel beams cannot be created to their full extend as they would carry an infinite amount of energy and require a non-finite aperture. This is also true for the presented radially self-accelerating beams, since they are a specific discrete superposition of Bessel beams. Another limitation arises from the fact that the Fourier-transform of a Bessel wave is a ring with infinitesimal thickness. In an experimental setting it is clear that only rings with finite width can be generated. As an immediate consequence, the range over which the experimentally generated beam resembles the theoretical prediction will be limited.

For experimental realization the set of parameters pre-

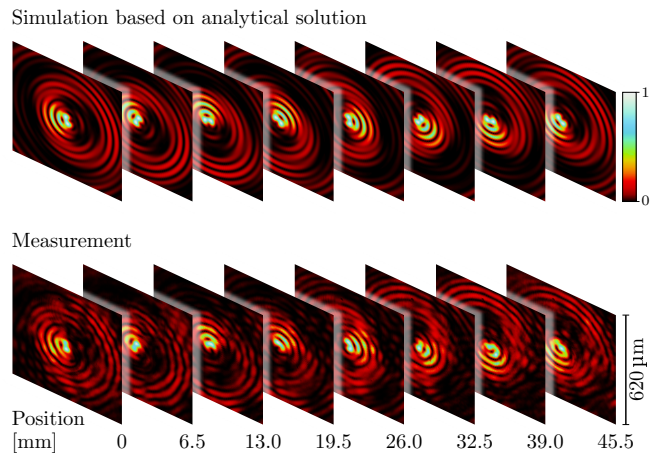


Figure 5. Simulation (top) and experimental results (bottom) showing the propagation dynamics of a radially self-accelerating beam identical to the one in Fig. 3. Radii on the SLM have been $R_1 = 2.328$ mm, $R_2 = 1.958$ mm and $R_3 = 1.501$ mm.

sented in Fig. 3 was used. For this purpose, a superposition of three rings was implemented in the SLM-plane. The subsequent Fourier-lens with focal length f connects the ring radii R_n on the SLM with the transverse components of the wave vector α_n via

$$\alpha_n = \frac{kR_n}{f}. \quad (11)$$

Fig. 5 shows an experimental scan along the propagation direction together with a simulation based on the analytical solution described by Eq. (8). In total, we were able to observe about two rotations over a length of 101.5 mm. See Supplemental Material at [URL will be inserted by publisher] for an animated representation of the full scan. The rotation rate was found to be $\omega_{\text{exp}} = (123.2 \pm 2.4) \frac{\text{rad}}{\text{m}}$ and is therefore in very good agreement with the intended value of $\omega_{\text{th}} = 125 \frac{\text{rad}}{\text{m}}$.

In conclusion, we have demonstrated the existence of a new class of self-accelerating waves. Theoretically, those waves, which accelerate freely on spiraling trajectories, were derived as solutions to the scalar Helmholtz equation. It was pointed out, that radially self-accelerating beams can be generated as a discrete superposition of Bessel waves with well defined properties. As such, they are quasi-non-diffractive, meaning that they are diffraction-free in a rotating, co-moving frame of reference. With the proposed experimental setup the study of beam properties under realistic conditions was shown to be possible with great flexibility. In a first proof of principle experiment, it was verified that the beam shows indeed the desired rotating behavior - yielding excellent agreement with the theoretical predictions - and, moreover, the transverse beam profile remains unbroadened for a substantially long propagation distance.

We foresee a broad range of applications for this new class of radially accelerating beams ranging from particle manipulation, e.g. as tractor beams, to material processing, e.g. photo lithography. In order to widen the range of possible applications even further, it is also of interest to study the properties of these kind of beams in more detail on a fundamental basis. For instance, with particle manipulation in mind, it is of great interest to investigate the self-healing behavior or the dynamics in random media. Regarding material processing, for example, the dynamics of such field configurations in non-linear environments is of great importance.

The authors wish to thank the German Ministry of Education and Research (Center for Innovation Competence program, grant 03Z1HN31), the Thuringian Ministry for Education, Science and Culture (Research group Space-time, grant no. 11027-514), the Deutsche Forschungsgemeinschaft (grant NO462/6- 1), and the German-Israeli Foundation for Scientific Research and Development (grant 1157-127.14/2011).

* Alexander.Szameit@uni-jena.de

- [1] G. A. Siviloglou, J. Broky, A. Dogariu, and D. N. Christodoulides, *Physical Review Letters* **99** (2007), 10.1103/PhysRevLett.99.213901.
- [2] G. A. Siviloglou and D. N. Christodoulides, *Optics Letters* **32**, 979 (2007).
- [3] M. A. Bandres, *Optics Letters* **33**, 1678 (2008).
- [4] A. Minovich, A. E. Klein, N. Janunts, T. Pertsch, D. N. Neshev, and Y. S. Kivshar, *Physical Review Letters* **107**, 116802 (2011).
- [5] J. Zhao, P. Zhang, D. Deng, J. Liu, Y. Gao, I. D. Chremmos, N. K. Efremidis, D. N. Christodoulides, and Z. Chen, *Optics Letters* **38**, 498 (2013).
- [6] I. Kaminer, J. Nemirovsky, K. G. Makris, and M. Segev, *Optics Express* **21**, 8886 (2013).
- [7] I. Kaminer, R. Bekenstein, J. Nemirovsky, and M. Segev, *Physical Review Letters* **108**, 163901 (2012).
- [8] F. Courvoisier, A. Mathis, L. Froehly, R. Giust, L. Furfaro, P. A. Lacourt, M. Jacquot, and J. M. Dudley, *Optics Letters* **37**, 1736 (2012).
- [9] J. Baumgartl, M. Mazilu, and K. Dholakia, *Nature Photonics* **2**, 675 (2008).
- [10] P. Polynkin, M. Kolesik, and J. Moloney, *Physical Review Letters* **103** (2009), 10.1103/PhysRevLett.103.123902.
- [11] I. Kaminer, M. Segev, and D. N. Christodoulides, *Physical Review Letters* **106**, 213903 (2011).
- [12] A. Lotti, D. Faccio, A. Couairon, D. G. Papazoglou, P. Panagiotopoulos, D. Abdollahpour, and S. Tzortzakos, *Physical Review A* **84**, 021807 (2011).
- [13] I. Dolev, I. Kaminer, A. Shapira, M. Segev, and A. Arie, *Physical Review Letters* **108**, 113903 (2012).
- [14] R. Bekenstein and M. Segev, *Optics Express* **19**, 23706 (2011).
- [15] E. Greenfield, M. Segev, W. Walasik, and O. Raz, *Physical Review Letters* **106**, 213902 (2011).
- [16] N. Voloch-Bloch, Y. Lereah, Y. Lilach, A. Gover, and A. Arie, *Nature* **494**, 331 (2013).
- [17] C. Paterson and R. Smith, *Optics Communications* **124**, 131 (1996).
- [18] J. Tervo and J. Turunen, *Optics Express* **9**, 9 (2001).
- [19] R. Vasilyeu, A. Dudley, N. Khilo, and A. Forbes, *Optics Express* **17**, 23389 (2009).
- [20] R. Rop, A. Dudley, C. Lopez-Mariscal, and A. Forbes, *Journal of Modern Optics* **59**, 259 (2012).
- [21] R. Rop, I. A. Litvin, and A. Forbes, *Journal of Optics* **14**, 035702 (2012).
- [22] D. B. Ruffner and D. G. Grier, *Physical Review Letters* **109**, 163903 (2012).
- [23] D. McGloin, V. Garces-Chavez, and K. Dholakia, *Optics Letters* **28**, 657 (2003).
- [24] P. Paakkonen, J. Lautanen, M. Honkanen, M. Kuittinen, J. Turunen, S. N. Khonina, V. V. Kotlyar, V. A. Soifer, and A. T. Friberg, *Journal of Modern Optics* **45**, 2355 (1998).
- [25] S. Chavez-Cerda, M. A. Meneses-Nava, and J. M. Hickmann, *Optics Letters* **23**, 1871 (1998).
- [26] J. A. Davis, D. M. Cottrell, J. Campos, M. J. Yzuel, and I. Moreno, *Applied Optics*, *Appl. Opt.* **38**, 5004 (1999).